ELSEVIER

Catalysis Today 59 (2000) 191–204

CATALYSIS TODAY

www.elsevier.com/locate/cattod

Preparation, characterization and reactivity of Me-hexaaluminate (Me=Mn, Co, Fe, Ni, Cr) catalysts in the catalytic combustion of NH_3-containing gasified biomasses

Luca Lietti*, Cinzia Cristiani, Gianpiero Groppi, Pio Forzatti

Dipartimento di Chimica Industriale ed Ingegneria Chimica "G. Natta", Politecnico di Milano, Piazza L. da Vinci 32, 20133 Milan, Italy

Abstract

The preparation, characterization and reactivity of metal-substituted (Mn, Cr, Co, Ni, Fe) hexaaluminate catalysts in the combustion of NH_3-containing gasified biomass-derived fuels is investigated. It is found that the preparation method adopted (carbonates route) is suitable to prepare microcrystalline matrices of high surface areas with high interspersion of the constituents. The calcination of all the microcrystalline matrices leads to the formation of a final monophasic materials with a Ba–β-Al_2O_3 structure and surface areas of 5–15 m^2/g. In these structures Ni is divalent and octahedrally and pseudo-octahedrally coordinated; Fe and Cr are trivalent in octahedral coordination and Co is both divalent tetrahedrally coordinated and trivalent octahedrally coordinated.

The prepared substituted hexaaluminate catalysts are active in the catalytic combustion of the biomass-derived fuels, and present different activity towards the various biogas components. In particular the Fe- and Mn-substituted samples show the highest activity in the combustion of methane, which is the least active biogas fuel. Over all the catalyst samples, ammonia contained in the biogas is oxidized to N_2 but large amounts of NO are also formed. However, the NO formation decreases at high temperatures: this phenomenon has been associated with the occurrence of a selective non-catalytic reduction (SNCR) process involving ammonia as reducing agent and occurring in the first part of the reactor in the simultaneous presence of oxygen, NO and ammonia.

Keywords: Catalytic combustion; Gasified biomasses; Ammonia oxidation; Me-substituted hexaaluminate catalysts; NO reduction; SNCR

1. Introduction

One of the major problems related to the production of energy through combustion processes is the emission of unwanted pollutants, i.e. CO_2 (responsible for the green-house effect), unburned hydrocarbons (UHCs), CO and NO_x. Accordingly, alternative low-pollution techniques for energy production are widely explored nowadays. In this respect, the catalytic combustion for gas-turbine (GT) applications has been extensively investigated in recent years because of its potential to minimize NO_x, UHC and CO emissions [1]. To date, natural gas is the most widely used fuel for catalytic combustion but the use of alternative (and possibly renewable) fuels with a lower environmental impact is of great interest. Among the proposed "renewable" fuels, those obtained by gasification of biomasses (biogas) are promising. Biogas has a complex composition, being constituted by CO, H_2, CH_4 and ethylene (Table 1). Large amounts of N_2 are also present when biogas is produced by gasification with air: in this case, the fuel is characterized by

* Corresponding author. Tel.: +39-02-2399-3272; fax: +39-02-7063-8173.
E-mail address: luca.lietti@polimi.it (L. Lietti)

0920-5861/00/$ – see front matter
PII: S0920-5861(00)00283-2

Table 1
Typical composition of gasified biomass fuel

Species	CO	H_2	CH_4	CO_2	H_2O	C_2H_4	N_2	NH_3	H_2S
mol%	15	10	5	14	11	1	44	0–0.3	0.01

low heating values and this may pose difficulties for its use in traditional gas turbines. This problem may be circumvented by the use of catalysts in gas turbines, which secure effective combustion by igniting and stabilizing the combustion reaction [2].

Several catalytic materials have been proposed for catalytic combustion. Among these, palladium-based catalysts are the catalyst of choice for natural gas-fueled GT combustors [1,3–6] since only these catalysts secure CH_4 ignition at reasonably low temperatures. Besides Pd-based catalysts, Mn-substituted hexaaluminate with alumina layered structure were considered to be promising for the combustion of H_2- or CO-containing fuels, due to the easier ignition of these components [7–11]. The use of Mn-substituted hexaaluminates as high temperature finishing catalysts has also been proposed in view of their excellent thermal stability [12].

The use of biogas in catalytic combustors may raise additional problems due to the presence of N- and S-containing compounds (such as NH_3 and H_2S, see Table 1) along with alkali compounds which may poison the catalyst. In a previous study from our group [13], the catalytic combustion of a NH_3-containing biogas has been investigated over both a Pd-based catalyst and a Mn-substituted hexaaluminate sample. It has been found that ammonia is easily oxidized over both catalyst samples, leading to the formation of significant amounts of NO_x. However, a significant reduction of the NO concentration has been observed at high temperature in the case of the Mn-substituted hexaaluminate sample, and this phenomenon has been associated with the occurrence of a gas-phase NO reduction by unconverted ammonia, according to the chemistry of the well-known selective non-catalytic reduction (SNCR) process.

In this work, the reactivity of other substituted hexaaluminate catalysts in the catalytic combustion of biogas fuel has been investigated, with particular emphasis to the occurrence of the ammonia oxidation reaction. Accordingly, Me-substituted hexaaluminate catalyst samples with nominal composition $BaMeAl_{11}O_{19}$ (where Me=Fe, Cr, Co, Ni and Cu) have been prepared according to the "carbonate" route previously proposed for the Mn-substituted catalysts. The obtained catalysts have been characterized and their reactivity in the oxidation of ammonia alone and in the presence of the biogas has been addressed, and results are reported in the following.

2. Experimental

2.1. Catalyst preparation

Samples with nominal composition $BaMeAl_{11}O_{19}$, where Me=Mn, Fe, Cr, Co, Ni and Cu, have been prepared using the "carbonate route". This method has been proposed in the literature to prepare both unsubstituted and substituted Ba–β-alumina samples with different compositions [8,14–16], and it is based on the coprecipitation in aqueous medium of carbonates and hydroxicarbonates of the constituent ions. In a typical preparation, a solution of the nitrates of the metal ions is prepared and the catalyst precursor is precipitated using a large amount of $(NH_4)_2CO_3$. The precipitation is carried out in an open flask at 60°C at constant pH (7–8), followed by aging of 3 h. Constant pH conditions are guaranteed by the buffer capability of the system.

The preparation of the $BaNiAl_{11}O_{19}$, $BaCoAl_{11}O_{19}$ and $BaCuAl_{11}O_{19}$ samples involved a few modifications of the general preparation procedure described above to avoid irreversible solubilization of Ni, Co and Cu ions. Indeed it is well known that Ni^{2+}, Co^{2+} and to a greater extent Cu^{2+} form in aqueous solution complex ions such as $[Me(NH_3)_4]^{2+}$ in the presence of excess NH_3 [17]. These complexes are soluble in a large range of pH, thus preventing the total precipitation of the metallic ions. Accordingly, in the case of Ni, Co, and Cu-containing materials, lower amounts of $(NH_4)_2CO_3$ have been used, corresponding to the stoichiometry of the formation of carbonates and hydroxides of the Al, Ba and Me metallic ions ($(NH_4)_2CO_3$/Ba=1; $(NH_4)_2CO_3$/Al=3; $(NH_4)_2CO_3/Me^{2+}$=2).

For all the samples, precipitation immediately occurs when the nitrates solution is poured in the carbonates one and a pH value in the range 7–8 is measured depending on the transition metal ion present in

the solution. The precipitation of the transition metal ion leads to the progressive discoloration of the supernatant solution and to the formation of a strongly colored precipitate (unsubstituted Ba–β-aluminas are white). In the case of the Ni, Co, and Cu-containing systems, colored mother liquors have been obtained upon filtration, indicating that a non-quantitative precipitation of the transition metal ions has occurred.

Chemical analyses by atomic absorption (VARIAN AA475 instrument) have been performed on the mother liquors of all the samples. The analyses have indicated that the precipitation of Ba and Al was quantitative, as well as that of Mn, Fe and Cr, whereas only minor amounts of Ni and Co ions were present in the mother liquors. Calculations have indicated that the Ni/Ba and Co/Ba atomic ratio were 0.95 and 0.96, respectively, i.e. very close to the nominal one (Me/Ba=1). In the case of Cu-containing material, large metal ion losses have been observed. Furthermore, upon calcination at 1300°C of the blue precursor of the Cu-substituted β-alumina, a white final material has been obtained, suggesting that Cu ions are no longer present in the structure, possibly due to the high volatility of Cu compounds [18]. Accordingly, the Cu-containing sample will not be further considered in the work.

The precursor materials obtained upon filtering the precipitate, washing and drying overnight at 110°C have been calcined at 500, 700, 900 1000, 1100, 1200 and 1300°C using a heating rate of 60°C/h, holding for 10 h at each temperature, followed by cooling down at a rate of 100°C/h.

In the following, the samples will be quoted using a notation that refers to the composition and the calcination temperature: e.g. BaCo-1000 indicates the sample with composition $BaCoAl_{11}O_{19}$ calcined at 1000°C.

2.2. Catalyst characterization

X-ray powder diffraction (XRD) patterns have been measured using Ni-filtered Cu Kα and a Philips Vertical Goniometer PW 1050-70 in the angular range 2θ=3–70°. Cell parameters have been calculated with a least square fitting routine, taking into account for systematic errors introduced by the goniometer.

UV–Visible–diffuse reflectance (UV–Vis–DR) spectra have been recorded by a Jasco spectrophotometer equipped with an integrating sphere and a reference of $BaSO_4$ (spectral range 250–850 nm; band width 4 nm).

Surface area (S_a) measurements have been accomplished by nitrogen adsorption with the BET method using a Fisons Sorptomatic 1900 series Instrument.

2.3. Catalytic activity tests

Catalytic activity experiments have been performed in a quartz tubular fixed bed microreactor (i.d. 7 mm) loaded with 0.128 g of catalyst having a particle diameter near 0.1 mm in order to reduce intraparticle diffusional limitations. The catalyst has been diluted with quartz granules of the same size (catalyst/quartz=2/1 w/w) to limit temperature gradients in the reactor. The reactor, which operated at P=120–140 kPa abs. due to pressure drops in the catalyst bed, has been inserted into an electric furnace driven by a PID temperature controller/programmer (Eurotherm 812). The temperature of the catalyst has been measured and controlled by means of a K-type thermocouple (o.d.=0.5 mm) sliding in a quartz thermocouple well (o.d.=2 mm) directly immersed in the catalyst bed.

The reactant gases, coming from calibrated gas cylinders (SAPIO), have been fed to the reactor by means of electronic mass-flow meter-controller (Brooks 5850 TR). The overall flow rate has been set at 120 cm^3/min (STP) (GHSV=56250 N cm^3/g_{cat} h).

The gases exiting the reactor have been analyzed by a quadrupole mass detector (Balzers QMS 200). The following mass-to-charge ratios (m/e) have been used to monitor the concentrations of products and reactants by the mass spectrometer: 2 (H_2), 15 (CH_4), 17 (NH_3), 18 (H_2O), 26 (C_2H_4), 28 (N_2, CO or C_2H_4), 30 (NO), 32 (O_2), 40 (Ar), 44 (N_2O or CO_2) and 46 (NO_2). The data have been quantitatively analyzed by taking into account the response factors and the overlapping of the fragmentation patterns experimentally determined. The analysis of N_2O, CO_2, N_2, C_2H_4 and CO has also been performed by a gas chromatograph (HP 5890) equipped with a Porapak Q and a 5 Å molecular sieve capillary column.

The catalytic oxidation of NH_3 has been investigated both in the absence and in the presence of the biogas fuels. In the first case, a stream of NH_3 (500 ppm)+O_2 (2% v/v)+Ar (3000 ppm, internal standard) in He (balance) has been fed to the reactor

Table 2
Phase composition of $BaMe_1Al_{11}O_{19}$ at different calcination temperatures[a]

Phase composition of samples						
T calculated (°C)	$BaAl_{12}O_{19}$	$BaMnAl_{12}O_{19}$	$BaCrAl_{11}O_{19}$	$BaFeAl_{11}O_{19}$	$BaCoAl_{11}O_{19}$	$BaNiAl_{11}O_{19}$
110	AACHH, Ba–Al	AACHH, MnCO, Ba–Al	AACHH, Ba–Al, Ba–Cr	AACHH, Ba–Al	AACHH	PSB
500	Amorphous	Amorphous	Amorphous	Amorphous	Amorphous	Amorphous
700	γ-Al_2O_3	α-Mn_2O_3, γ-Al_2O_3	γ-Al_2O_3, $BaCrO_4$	γ-Al_2O_3	γ-Al_2O_3	γ-Al_2O_3
900	γ-Al_2O_3, $BaAl_2O_4$	α-Mn_2O_3, γ-Al_2O_3, $BaAl_2O_4$	γ-Al_2O_3, $BaCrO_4$, $BaAl_2O_4$	γ-Al_2O_3, $BaAl_2O_4$	γ-Al_2O_3	γ-Al_2O_3, $BaAl_2O_4$
1000	γ-Al_2O_3, $BaAl_2O_4$	γ-Al_2O_3, $BaAl_2O_4$, Ba–β-Al_2O_3	γ-Al_2O_3, $BaCrO_4$, $BaAl_2O_4$	$BaAl_2O_4$, Ba–β-Al_2O_3 tr	γ-Al_2O_3, $BaAl_2O_4$ tr	γ-Al_2O_3
1100	γ-Al_2O_3, $BaAl_2O_4$, Ba–β-Al_2O_3	Ba–β-Al_2O_3	Ba–β-Al_2O_3, $BaCrO_4$, $BaAl_2O_4$	$BaAl_2O_4$, α-Al_2O_3, Ba–β-Al_2O_3	Ba–β-Al_2O_3, $BaAl_2O_4$ tr	Ba–β-Al_2O_3
1200	Ba–β-Al_2O_3, $BaAl_2O_4$ tr	Ba–β-Al_2O_3	Ba–β-Al_2O_3, $BaCrO_4$, $BaAl_2O_4$	Ba–β-Al_2O_3	Ba–β-Al_2O_3	Ba–β-Al_2O_3
1300	Ba–β-Al_2O_3	Ba–β-Al_2O_3	Ba–β-Al_2O_3	Ba–β-Al_2O_3	Ba–β-Al_2O_3	Ba–β-Al_2O_3

[a] AACHH=$(NH_4)_2Al_6(OH)_{14}(CO_3)_3{\cdot}H_2O$; Ba–Al=$BaAl_2(CO_3)_2(OH)_4{\cdot}H_2O$ and/or $Ba_2Al_4(OH)_{16}$; Ba–Cr=$BaCr_2O_7$, $BaCrO_3$ and/or $Ba_5OH(CrO_4)_3$, PSB=pseudo-bohemite, tr=trace amounts.

at room temperature. After the mass-spectrometer signals had stabilized, the catalyst temperature has been linearly increased at 7°C/min up to 950°C, while continuously monitoring the concentration of the gases exiting from the reactor. When the catalytic oxidation of NH_3 has been investigated in the presence of the biogas fuels, a stream composed by NH_3 (500 ppm), CO (5000 ppm), CH_4 (1800 ppm), H_2 (3800 ppm), C_2H_4 (300 ppm), Ar (3000 ppm), O_2 2% and He (balance) has been used. Total flow rate and other experimental conditions were as those used for NH_3 oxidation. It is worth to note that the composition of the fuel mixture used in this study closely resembles that of a typical biogas-fueled catalytic combustor, but diluted by a factor of 7. Such dilution has been used to reduce the temperature gradients in the reactor.

All the experiments have been duplicated to check for any irreproducibility, but very similar results have been always obtained. N- and C-balances were usually close within ±5%, being usually near ±3%. Only the N-balances performed at low temperatures when ammonia is present do not fall within the above limits due to the transient desorption of NH_3.

3. Results

3.1. Chemico-physical characterization

The phase composition of the various investigated samples detected by XRD at different temperatures are reported in Table 2.

The BaMn, BaFe, BaCr, BaNi and BaCo samples dried at 110°C evidence quite a complex phase composition. Indeed, except for BaNi-110 that is completely amorphous, in all the other samples the presence of crystalline $(NH_4)_2Al_6(OH)_{14}(CO_3)_3{\cdot}H_2O$ (ammonium aluminum carbonate hydroxy-hydrate, AACHH), and of crystalline mixed Ba–Al compounds (tentatively $BaAl_2(CO_3)_2(OH)_4{\cdot}H_2O$ and $Ba_2Al_4(OH)_{16}$ [14,15]) has been pointed out. In the case of the BaCr-110 sample, Ba–Cr mixed compounds are also present (tentatively $BaCrO_3$, $BaCr_2O_7$, $Ba_5OH(CrO_4)_3$ [19]).

All these crystalline phases decompose upon calcination at 500°C to give, for all the samples, amorphous materials that are still amorphous or microcrystalline upon calcination at 700°C. At this temperature, only modulations of the XRD base line

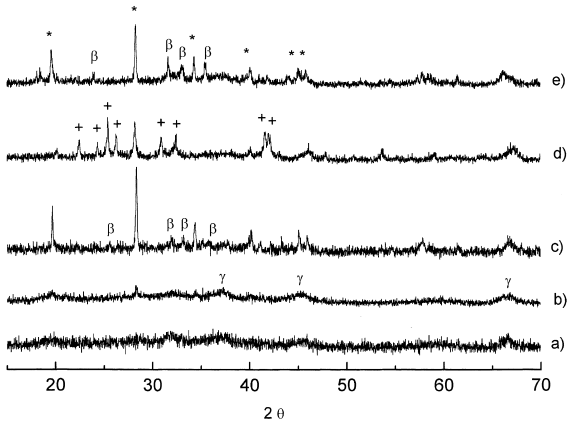

Fig. 1. XRD spectra of samples calcined at 1000°C: (a) BaNi; (b) BaCo; (c) BaFe; (d) BaCr; and (e) BaMn. Symbols: (*) $BaAl_2O_4$, (+) $BaCrO_4$, (β) Ba–β-Al_2O_3, (γ) γ-Al_2O_3.

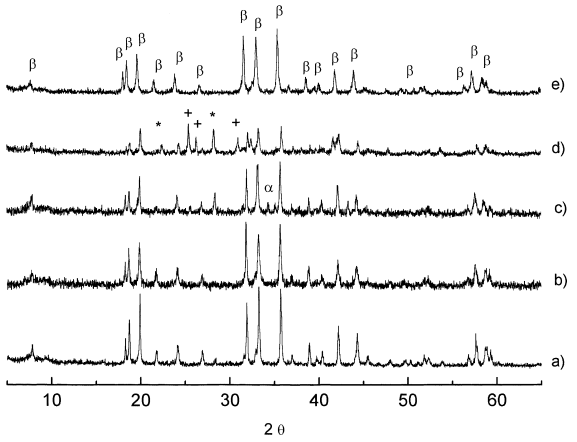

Fig. 2. XRD spectra of samples calcined at 1100°C: (a) BaNi; (b) BaCo; (c) BaFe; (d) BaCr; and (e) BaMn. Symbols: (*) $BaAl_2O_4$, (+) $BaCrO_4$, (β) Ba–β-Al_2O_3, (α) α-Al_2O_3.

ascribable to γ-Al_2O_3 [JCPDS 10-425] are observed for all the samples, along with traces of α-Mn_2O_3 [JCPDS 10-69] and $BaCrO_4$ in the case of BaMn- and BaCr-700 samples, respectively.

Calcination at 900°C induces the formation of crystalline $BaAl_2O_4$ [JCPDS 17-306] in traces in BaNi-900, and in extensive amounts in BaFe, BaMn, and BaCr-900 samples. In this last catalyst, the progressive crystallization of $BaCrO_4$ is also observed. The smooth base line modulations in the XRD spectra associated with the presence of γ-Al_2O_3 matrix are also present in all the samples.

The XRD spectra of the investigated samples calcined at 1000°C are reported in Fig. 1. In the BaCr, BaCo, and BaNi-1000 samples, no significant differences are apparent if compared with the spectra recorded at 900°C, whereas in BaFe- and BaMn-1000, small amounts of Ba–β-Al_2O_3 (JCPDS 26-135) are also formed. For all the samples, no evidence of transition of γ-Al_2O_3 to δ, θ, or α-phases is detected. It is worth to note that the formation of the Ba–β-Al_2O_3 phase in unsubstituted systems occurs at 1100°C [14], i.e. 100°C above that observed for BaMn and BaFe.

Calcination at 1100°C leads in all the samples to the formation of the final Ba–β-Al_2O_3 phase (Fig. 2), which is accompanied by the progressive disappearance of the other Ba-containing phases ($BaAl_2O_4$ and $BaCrO_4$). At this temperature, the BaCo, BaMn and BaNi-1100 samples are practically monophasic, while minor amounts of $BaAl_2O_4$ and α-Al_2O_3 are present in BaFe-1100, and of $BaCrO_4$ in BaCr-1100.

All the samples become monophasic upon calcination at 1200°C with the exception of BaCr in which traces of $BaCrO_4$ are still evident. This sample becomes monophasic only upon calcination at 1300°C: at this temperature (Fig. 3), all the samples consist of a $BaMeAl_{11}O_{19}$ phase with a Ba–β-Al_2O_3 structure.

As reported elsewhere [14], this structure consists of alternate stacking along the *c* axis of Al^{3+}-containing spinel blocks and mirror planes in which the large Ba^{2+} cations are located. Calculated cell parameters

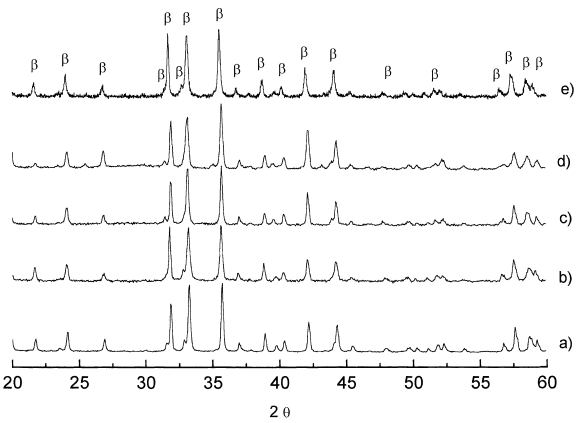

Fig. 3. XRD spectra of samples calcined at 1300°C: (a) BaNi; (b) BaCo; (c) BaFe; (d) BaCr; and (e) BaMn. Symbols: (β) Ba–β-Al_2O_3.

Table 3
Calculated cell parameters for different $BaMeAl_{11}O_{19}$

Sample	$a_0=b_0$ (Å)	c_0 (Å)
$BaAl_{12}O_{19}$[a]	5.5936(4)	22.767(2)
$BaMnAl_{11}O_{19}$[a]	5.64123(4)	22.7260(3)
$BaCrAl_{11}O_{19}$	5.624(6)	22.90(3)
$BaFeAl_{11}O_{19}$	5.633(9)	22.88(4)
$BaCoAl_{11}O_{19}$	5.628(3)	22.68(1)
$BaNiAl_{11}O_{19}$	5.622(7)	22.73(3)

[a] Determined by Rietveld analysis.

of the BaMe-1300 samples are reported in Table 3 and compared with those of the unsubstituted $BaAl_{12}O_{19}$ sample. The calculated value of the a_0 cell parameter in the Me-containing materials is always larger than that of the unsubstituted one. This points out that the larger Mn, Cr, Fe, Co, and Ni ions are allocated in the final structure replacing the smaller Al^{3+} ions. A more complex behavior is observed for c_0 that are either larger or smaller than in the unsubstituted sample depending on the transition metal ion. A previous detailed investigation on the structure of Mn-substituted hexaaluminates [16] pointed out that, to maintain electroneutrality, the replacement of Al^{3+} with Mn^{2+} ions in the structure results in an increase of the Ba concentration in the mirror plane. It was also observed that the increase of the Ba concentration enforced the bonds between the spinel blocks and the mirror plane. This results in a contraction of the mirror plane and, consequently, in a decrease of c_0. It is worth to note that this effect is not observed when the Al^{3+} ions are replaced by ions having the same oxidation state (e.g. Mn^{3+}) [16]. Accordingly calculated values of c_0 suggest that in Mn, Co and Ni-substituted samples, that exhibit smaller c_0 than the unsubstituted material, the Me ion preferentially enters the structure with 2+ oxidation state, whereas in Cr- and Fe-substituted samples the Me ion preferentially enters the structure with 3+ oxidation state.

To collect further indications on the oxidation state and coordination of the transition metal ions incorporated in the Ba–β-Al_2O_3 structure, UV–Vis–DR analyses have been performed. The obtained spectra are reported in Fig. 4a–d. The spectrum of BaNi-1300 is quite complex (Fig. 4a), being characterized by two strong absorptions centered at about 300 and 600 nm that are accompanied by many shoulders. The major bands can be attributed to the spin-allowed (380, 580, 645 and 720 nm) and spin-forbidden (425 and 770 nm) d–d transitions of Ni^{2+} in octahedral coordination [20,21]. In the spectrum of BaCo-1300 (Fig. 4b) the complex convolution centered at about 600 nm is associated with the presence of both Co^{2+} and Co^{3+} ions. Indeed, the bands at 410 and 600 nm correspond to d–d transitions of Co^{2+} tetrahedrally coordinated and those at 455, 480, 550 and 645 nm are characteristic of the d–d transitions of Co^{3+} ions in octahedral coordination [22]. In the spectrum of BaFe-1300 (Fig. 4c), the characteristics bands of the $O^{2-}\rightarrow Fe^{3+}$ charge transfer at 300 nm and the d–d transitions of octahedrally coordinated Fe^{3+} ions at 380, 460, 520 and 550 nm are observed [16]. In view of the absence of the typical absorption bands at 610 and 690 nm due to d–d transitions of Fe^{2+} in tetrahedral coordination, and also of the absence of the intervalence charge transfer band at 730–740 nm (always observed when both Fe^{2+} and Fe^{3+} species are present [16]), the presence of Fe^{2+} ions in this sample has been excluded. Finally, in the BaCr-1300 UV–Vis–DR spectrum (Fig. 4d), the bands at 370, 420, 570 and 595 nm can be attributed to d–d transitions of Cr^{3+} in octahedral coordination [23].

The samples dried at 110°C evidence high surface areas in the range 200–300 m^2/g. Surface area values are not markedly affected by calcination treatment up to 700°C: in line with the microcrystallinity of the samples, values of 150–200 m^2/g are still observed at this temperature. A progressive but slow decrease in the surface area values is observed upon calcination of the samples at higher temperatures: after calcination at 1000°C, surface areas decrease to 70–100 m^2/g. Upon calcination at 1100°C, a marked drop in surface area values is observed (15–30 m^2/g), associated with the incipient formation of the final Ba–β-Al_2O_3 phase. Surface area values further decrease to 5–15 m^2/g upon calcination at 1300°C. These values are in line with those reported in the literature for similar materials prepared via alkoxides hydrolysis [24].

3.2. *Reactivity of $BaMeAl_{11}O_{19}$ in the combustion of ammonia and of the biogas*

Fig. 5a–d report the concentration profiles of the N-derived compounds recorded as a function of tem-

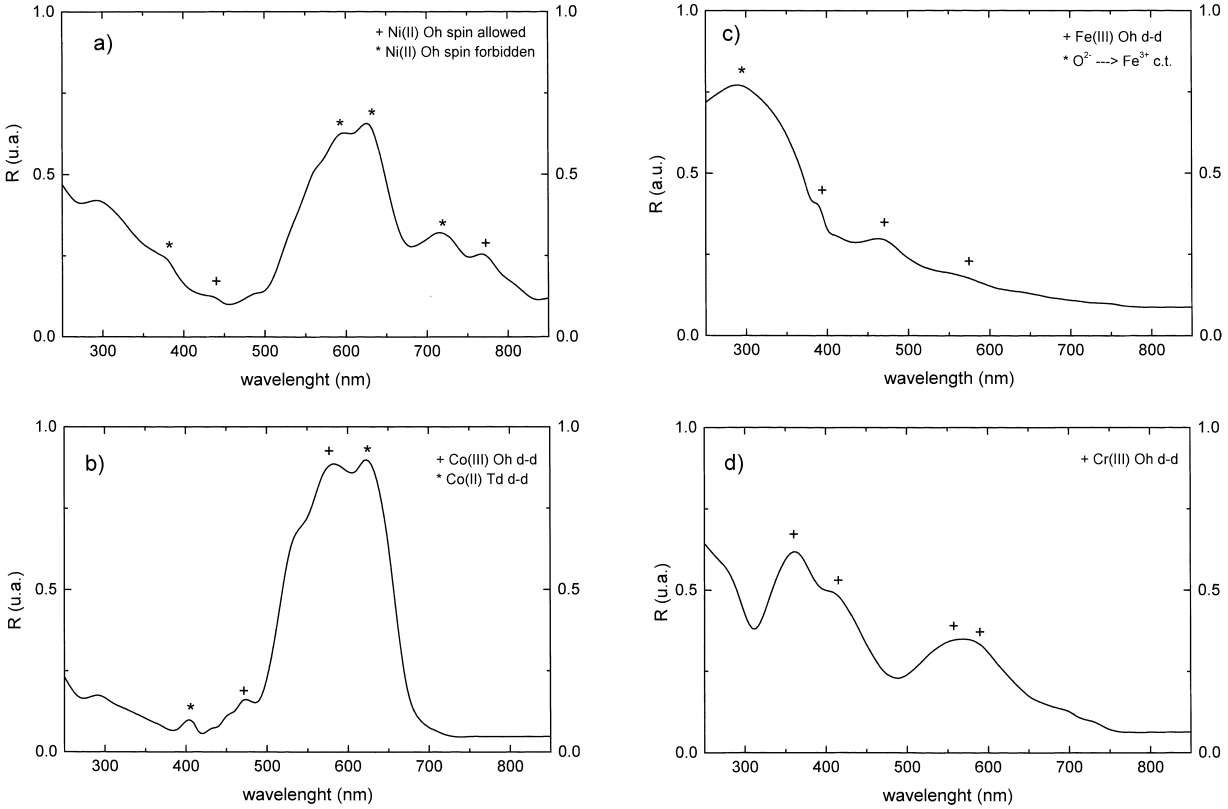

Fig. 4. UV–Vis–DR spectra of (a) BaNi-1300; (b) BaCo-1300; (c) BaFe-1300; and (d) BaCr-1300.

perature during the ammonia oxidation experiments performed over the $BaMeAl_{11}O_{19}$ catalysts calcined at 1300°C.

In the case of the Mn- and Cr-hexaaluminate catalysts, the ammonia concentration profile with temperature exhibits quite a complex behavior (Fig. 5a), showing a maximum at low temperatures due to the desorption of adsorbed ammonia species and then a decrease above 250–300°C due to its consumption. In the case of the other catalyst samples, i.e. the Fe, Co, and Ni-substituted samples, the initial NH_3 concentration peak is not observed, possibly due to the lower amount of ammonia adsorbed on the catalyst surface at room temperature. Complete NH_3 consumption is attained near 500°C in the case of the BaFe-1300 and BaMn-1300 samples, and near 600–650°C for the other investigated catalysts. In all cases, main reaction products are NO (Fig. 5b) and N_2 (Fig. 5c); significant amounts of N_2O have also been observed in the case of the BaMn-1300 sample only, and to a minor extent in the case of the BaCr sample (Fig. 5d).

For all catalysts, NO is produced above 300°C; its concentration exhibits a broad maximum in the temperature range 600–800°C. N_2 is formed above 250°C, but in lower amounts. Over all the catalyst samples, the N_2 concentration shows a maximum near 400–500°C and then an increase at high temperature, above 700–800°C. The maximum near 400–500°C is weak in the case of the Mn- and Cr-substituted samples, whereas it is well evident for the other catalysts. It is worth to note that the increase in the N_2 concentration profile that is observed at high temperatures is specular to the decrease of the NO concentration trace, where complete NH_3 conversion is achieved. The formation of the NH_3 oxidation products is also accompanied by the evolution of water, not reported in the figures.

The ammonia oxidation reaction was also carried out in the presence of the biomass derived fuels,

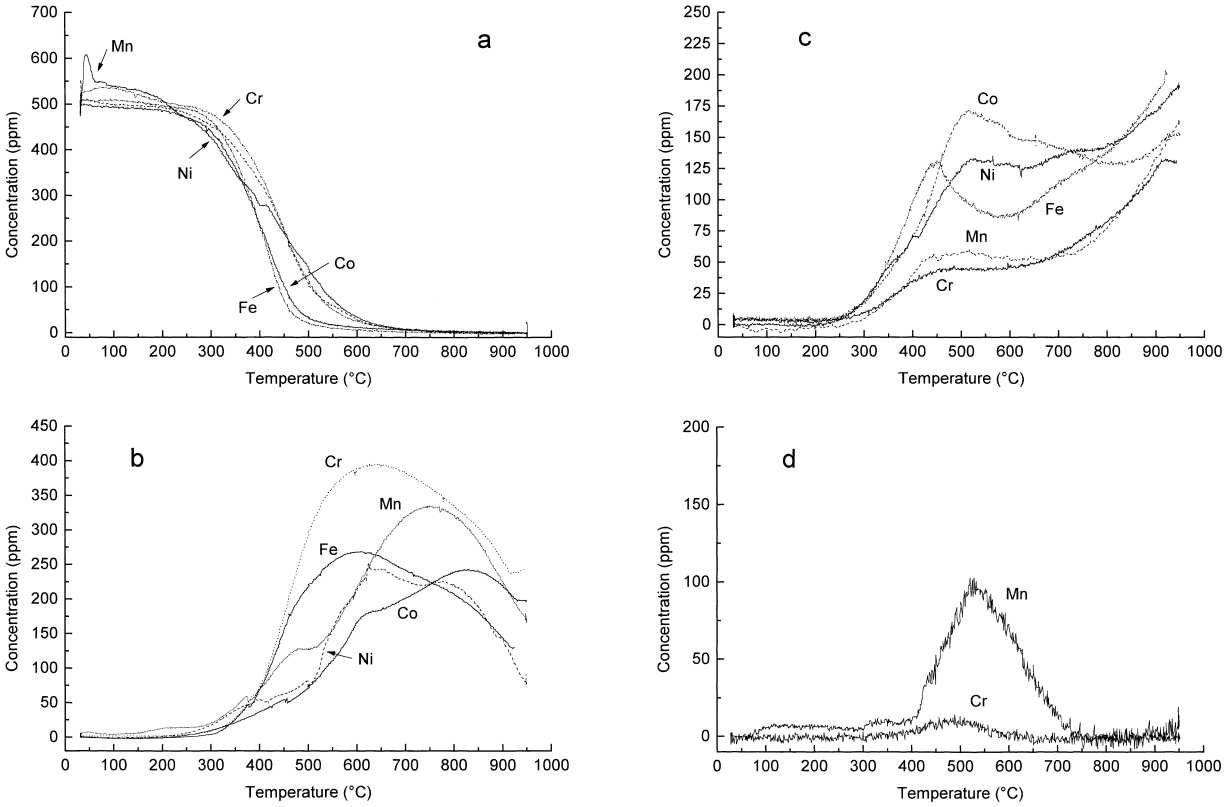

Fig. 5. Results of ammonia oxidation reaction performed over the $BaMeAl_{11}O_{19}$ catalysts (Me=Mn, Ni, Cr, Fe, Co). Concentration of (a) NH_3; (b) NO; (c) N_2; (d) N_2O. Feed: NH_3 500 ppm, O_2 2%, He balance.

and results have been displayed in Fig. 6a (CH_4 conversion) and b (NO concentration) as a function of temperature. Methane, which is the least reactive fuel component in the biogas mixture, is ignited at temperatures in the range 550–700°C. The Mn- and Fe-substituted hexaaluminates show the highest activity in the combustion of methane, in line with results previously reported by Machida et al. [24]. Over these catalysts CH_4 is converted starting from 550–600°C and complete conversion is achieved at 800°C. The reactivity of the Co- and Cr-substituted samples is slightly lower whereas the $BaNiAl_{11}O_{19}$ catalyst exhibits a different behavior in that it shows the highest light-off temperature but a very steep methane conversion curve with temperature, possibly related to the homogeneous ignition of the fuels. CO and H_2 (not reported in the figures) are oxidized at lower temperatures when compared to methane. Both fuels show an ignition temperature near 300°C over all catalyst samples, with the exclusion of the Ni-substituted catalyst which exhibits a very poor reactivity towards CO below 750°C.

Concerning the ammonia-derived products originating from the simultaneously occurring NH_3 oxidation reaction, the concentration profiles of NO obtained in the presence of the fuel mixture are displayed in Fig. 6b. These profiles roughly resemble those obtained in the absence of the fuels (Fig. 5b), in that a maximum is still present in all cases in the temperature range 600–800°C. However in these cases the maximum is more pronounced since a more rapid decrease in the NO concentration is evident above 750°C for all catalysts, accompanied by a parallel formation of N_2 (not reported in the figure) which in this case has been detected by GC analysis due to the overlapping with CO, present in the mixture in much higher amounts. Minor amounts of N_2O have also been observed near 500°C in the case of the BaMn-1300 catalyst sample only.

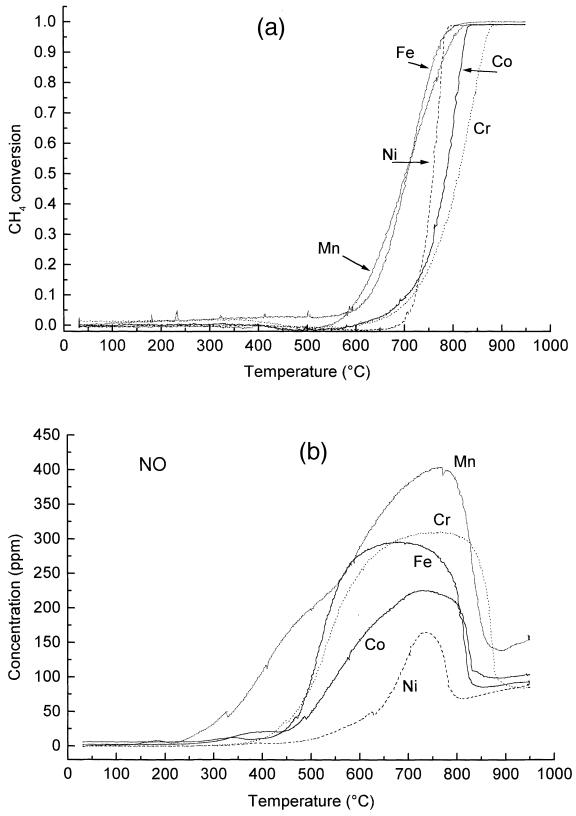

Fig. 6. Results of biogas oxidation reaction performed over the $BaMeAl_{11}O_{19}$ catalysts (Me=Mn, Ni, Cr, Fe, Co). (a) CH_4 conversion; and (b) NO concentration. Feed: NH_3 500 ppm, CO 5000 ppm, CH_4 1800 ppm, H_2 3800 ppm, C_2H_4 300 ppm, CO_2 5000 ppm, O_2 2%, He balance.

4. Discussion

4.1. Preparation and characterization of $BaMeAl_{11}O_{19}$ catalysts

It is evident that the preparation method here adopted (carbonates route) is suitable to prepare systems of composition $BaMeAl_{11}O_{19}$ in which the Me ion is allocated in the final Ba–β-Al_2O_3 structure. This method takes advantage from its simplicity since, starting from high-soluble inorganic precursors of the metal ions (e.g. nitrates), it operates in aqueous medium and in open flasks. Precipitation is conveniently performed with ammonium carbonate due to the low solubility of the hydroxy-carbonate precursors obtained during precipitation. It has been found that to obtain a quantitative precipitation of the metal ions, it is necessary to operate with suitable amounts of the precipitating agent in view of the different chemical behavior of the Me ions. Excess of $(NH_4)_2CO_3$ can be used to precipitate Fe, Mn and Cr, whereas stoichiometric amounts must be used for Ni and Co due to the formation of ammonium complexes which prevent quantitative precipitation of these ions. It is worth to note that when nitrates solution is poured in the carbonate one, the precipitation reaction occurs at constant pH=7–8 due to the buffer capability of the system. Failure in preparation of Cu-containing material can be ascribed to both the precipitation method and to the high temperatures required upon calcination for the formation of the Ba–β-Al_2O_3 structure.

Considering that in previous studies unsubstituted $BaAl_xO_{(2+3x)/2}$ (with x=9, 12 and 14) [14], substituted $BaMn_yAl_{12-y}O_{19}$ (with y=0.5, 1, 2 and 3) [8,15] and $BaFe_zAl_{12-z}O_{19}$ (with z=3, 9 and 12) [16] systems have been obtained using the same coprecipitation method here adopted, it can be concluded that this method represents a suitable route for the preparation of materials characterized by Ba–β-Al_2O_3 structure with good sintering resistance and morphological properties at high temperatures.

The thermal evolution of $BaMeAl_{11}O_{19}$ systems is analogous to that previously reported for samples of similar compositions [8,14–16]. All the samples dried at 110°C consist of an amorphous matrix and of crystalline Ba- and/or Al-containing materials that easily decompose upon calcination at 700°C. At this temperature the samples are characterized by high surface area values (150–200 m^2/g) and consist of a microcrystalline γ-Al_2O_3 phase. At higher temperatures (900–1000°C), the formation of crystalline $BaAl_2O_4$ is observed, while despite the high calcination temperature no formation of sintered alumina phases such as θ- or α-Al_2O_3 is detected. The formation of the Ba–β-Al_2O_3 final phase is observed starting from 1000°C for the Fe- and Mn-containing samples, and at 1100°C for the other materials. The formation is in all cases completed after calcination at 1300°C. At this temperature, monophasic materials with Ba–β-Al_2O_3 are obtained for all the samples in which the Me transition metal ion is incorporated in the structure.

In previous studies on Me-free samples ($BaAl_x$-$O_{(2+3x)/2}$ with x=9, 12, 14) prepared via the same

route [14], it has been proposed that the formation of the Ba–β-Al_2O_3 phase proceeds through simultaneous solid state reactions involving amorphous Ba species and γ-Al_2O_3 on one side and $BaAl_2O_4$ with γ-Al_2O_3 on the other side. The presence of amorphous Ba species has been invoked in view of the results of quantitative XRD analyses indicating that only 30% of the total Ba is involved in the formation of the $BaAl_2O_4$ phase [13]. The key factor for the achievement of the final monophasic material with high surface area has been reported to be the presence of highly interspersed Ba species which hinders alumina transitions until the formation of the final phase. A temperature threshold of 1100°C has been found for the formation of the Ba–β-Al_2O_3 phase: this temperature threshold has been related to the activation of the mobility and diffusion of Ba ions into the γ-Al_2O_3 spinel blocks.

An analogous mechanism of formation has been found to operate in the case of the $BaMn_yAl_{12-y}O_{19}$ (y=0.5–3) system [15] and can also be reasonably hypothesized for the formation of the Ba–β-Al_2O_3 structure in the Me-substituted materials investigated in this work. Also in this case, in spite of the formation of crystalline $BaAl_2O_4$, the presence of dispersed Ba species can be invoked considering that in all the samples no γ-→θ-→α-Al_2O_3 transitions of the γ-Al_2O_3 matrix has been observed even upon calcination at high temperatures. Such a high interspersion originates from the adopted precipitation conditions that results in amorphous or very microcrystalline domains where Ba and Al are interspersed at the atomic level. In the Cr, Co and Ni-containing samples a temperature threshold near 1100°C has been observed for the formation of the Ba–β-Al_2O_3 phase, like in the unsubstituted samples, whereas in the case of the Mn-containing samples the onset of the transformation is seen at 1000°C. Besides, traces of Ba–β-Al_2O_3 are observed also for the BaFe-1000 sample. A promoting effect of the transition metal ion for the formation of the Ba–β-Al_2O_3 phase has been already reported for $BaMn_yAl_{12-y}O_{19}$ systems [15]. The shift towards lower temperature of the onset for the formation of the final phase has been related to the increased ion mobility within the γ-Al_2O_3 spinel blocks. Mn ions can accelerate the γ-Al_2O_3 phase transitions, that are associated with lattice rearrangements requiring oxygen ion mobility [15]. A minor promoting effect can be hypothesized also for Fe ions, whereas no effect is apparent for the other transition metal ions, i.e. Co, Ni and Cr.

The formation of the Ba–β-Al_2O_3 phase is completed upon calcination at 1300°C. At this temperature, monophasic materials with the Ba–β-Al_2O_3 structure are obtained for all the samples. The Ba–β-Al_2O_3 phase can accommodate foreign ions in the structure replacing the Al^{3+} cations in both the tetrahedral and octahedral coordination [7], as indeed observed in the case of Mn-containing system [15]. It has been shown that Mn is present in the structure as Mn^{3+} and Mn^{2+} cations, in octahedral and tetrahedral coordination, respectively. As mentioned above the replacement of Al^{3+} by Mn^{2+} is allowed by a charge compensation mechanism which can operate due to presence of cations vacancies in the mirror planes of the structure [15]. In the Me-substituted samples, the Co, Fe, Ni and Cr ions are allocated in the Ba–β-Al_2O_3 structure replacing the Al^{3+} ions, as pointed out by the enlargement of the a_0 lattice parameter. Besides the values of calculated c_0 suggest that the Me ion preferentially enter the structure in divalent oxidation state in Co, Ni, and Mn-substituted samples and in trivalent oxidation state in Cr- and Fe-containing materials. These results are in line with literature report on the average oxidation state of transition metal ions in Ba–β-Al_2O_3 obtained by TPR experiments [24].

Further evidences on the oxidation state and coordination of the foreign ions have been provided by UV–Vis–DR. Although the assignments cannot be considered as definitive due to the broadness of the spectra and of the large overlapping of the characteristic bands of the single species, the analysis of the UV–Vis–DR spectra suggests that Ni^{2+}, Cr^{3+} and Fe^{3+} are allocated in octahedral sites, whereas Co^{2+} and Co^{3+} are accommodated in tetrahedral and octahedral coordination, respectively. These attributions are consistent with literature data [25].

4.2. Reactivity of $BaMeAl_{11}O_{19}$ catalysts in the catalytic combustion of ammonia and of the biogas fuels

The results presented in Figs. 5 and 6 show that, over all the investigated $BaMeAl_{11}O_{19}$ catalyst samples, significant amounts of NO are formed upon com-

bustion of both NH_3 and NH_3-containing fuels. In this respect, the investigated Me-substituted hexaaluminate catalysts show qualitatively similar results: this points out that the chemistry of the ammonia oxidation over these catalysts is similar and nearly independent on the transition metal ion present in the catalyst structure. Notably, similar results have also been reported by Johansson and Järås [26] over similar catalysts. These data contrast with the low-NO_x emissions requirements of gas-turbine applications; however, an interesting feature emerging from our results is that the NO concentration significantly decreases at high temperatures, and a parallel formation of molecular nitrogen is observed. As a matter of fact, N_2 selectivities up to 80% have been measured in a few cases. Notably, the N_2 formation is not thermodynamically limited due to the favorable thermodynamic equilibrium which favors the N_2 formation in the whole temperature range. The decrease of the NO concentration is even more pronounced when the ammonia oxidation reaction is carried out in the presence of the biogas fuels. This aspect is of relevance for practical applications since it may suggest, in principle, the possibility of reducing the NO emissions when operating under proper operating conditions.

In a previous paper from our group [13], the reasons explaining the decrease in the NO concentration observed at high temperatures over the $BaMnAl_{11}O_{19}$ catalyst sample have been addressed. In particular, various possibilities for the decrease of the NO concentration have been addressed, including: (i) the occurrence of a NO decomposition reaction, either homogeneous or catalytic; (ii) a specific reduction by one of the fuels present in the biogas mixture; and (iii) a specific selective behavior of the catalyst which at high temperatures favors the N_2 formation with respect that of NO.

The feasibility of the NO decomposition reaction was readily ruled out on the basis of specific experiments [13]. Concerning (ii), the reactivity of NO in the presence of various reductants (e.g. CO, H_2, CH_4, C_2H_4) has been investigated both in the presence of the catalyst and in the gas-phase as well, in the presence and in the absence of oxygen. The results of these experiments indicated that in the presence of oxygen no one of the biogas component is able to reduce NO, neither in the gas-phase nor in the presence of the $BaMnAl_{11}O_{19}$ catalyst [13]. Indeed the various fuels are readily oxidized by oxygen without showing any reducing capability towards NO, thus ruling out the occurrence of either a catalytic or homogeneous reduction reaction. Along similar lines, a specific catalyst behavior which favor the N_2 selectivity at high temperature (iii) is, in our opinion, not very likely. On the other hand, experiments performed with NH_3+NO mixtures indicated that ammonia itself, i.e. the NO precursor, is able to reduce NO at high temperatures (above 800°C) in the gas phase according to the stoichiometry of the well-known homogeneous $DeNO_x$-SNCR process, viz:

$$4NO + 4NH_3 + O_2 \rightarrow 4N_2 + 6H_2O \quad (1)$$

According to literature indications, this process involves the formation of an amide radical $NH_2^\bullet$ which then reacts with gas-phase NO giving rise to N_2 [27]. The $NH_2^\bullet$ radical is originated from ammonia via $H^\bullet$ abstraction by radicals such as $OH^\bullet$ and $O^\bullet$, which are present in an oxidizing environment [28]. If proper operating conditions are not established, the $NH_2^\bullet$ radical may either not form (i.e. ammonia does not react) or be over-oxidized to N_2 and/or NO. Hence a characteristic temperature window for the occurrence of the SNCR process does exist. The data reported in [13] clearly indicate that suitable conditions for the occurrence of this reaction are achieved during our experiments, thus suggesting that the decrease in the NO concentration observed at high temperature during the NH_3 oxidation experiments (Figs. 5 and 6b) may be related to the occurrence of reaction (1). It is worth to note that the occurrence of the SNCR process (1) requires the simultaneous presence, in the gas-phase and at high temperatures, of ammonia, NO and oxygen. In the case of the NH_3 oxidation experiments reported above, where ammonia and oxygen but no NO are fed to the reactor, it is speculated that NO is reduced by NH_3 at high temperature according to a gas-phase NO-SNCR process since suitable conditions for the occurrence of the SNCR reaction are reached in the first part of the reactor, where NO is already formed (via surface-catalyzed NH_3 oxidation) and unreacted ammonia is still present in the gas-phase.

The hypothesis of the occurrence of a NO-SNCR process by ammonia is also supported by the observation that in the presence of the biogas fuel components a more rapid decrease in the NO concentration is observed at high temperatures (compare Figs. 5b with

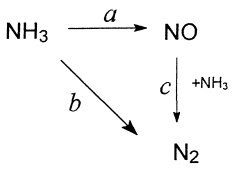

Scheme 1. Simplified reaction scheme for NH_3 oxidation over $BaMeAl_{11}O_{19}$ catalysts.

6b), in line with the well known promoting effects of fuels like CO and H_2 on the SNCR process [28,29]. In fact, in line with literature indications [28,30,31], it is likely that the enhancement of the SNCR process observed in the presence of the biogas is not due to a direct NO reduction by the fuels (as indeed proved by the NO reduction experiments reported in [13]), but relays on an increase of the radical pool by fuel oxidation [32].

Accordingly, in view of the similarity of the NH_3 oxidation chemistry previously invoked for all the $BaMeAl_{11}O_{19}$ catalysts, it is speculated that also for the Fe, Co, Ni and Cr-hexaaluminate samples the occurrence of the NO-SNCR process by NH_3 may be responsible for the observed decrease of the NO concentration at high temperature.

Hence, on the basis of the data reported above, the simplified reaction Scheme 1 (which neglect the formation of N_2O) can be sketched to represent the chemistry of the ammonia oxidation over the investigated Me-hexaaluminate catalysts.

In Scheme 1, routes *a* and *b* represent the direct NH_3 oxidation to NO and N_2, respectively. These reactions effectively occur on the catalyst surface already at low temperatures (i.e. near 300°C, Fig. 4), but hardly occur in the gas-phase under our experimental conditions as confirmed by activity runs performed in the empty reactor with NH_3+O_2 mixtures [13].

Route *c* represents the occurrence of NO reduction processes. On the basis of the results of the NO reduction experiments reported in [13] (and briefly summarized above) and in line with other literature data [28], only ammonia in the presence of oxygen has the capability of reducing NO according to the stoichiometry of the SNCR reaction (1). The occurrence of the SNCR process requires, as previously reported, the simultaneous presence of NH_3, NO and oxygen: it is speculated that this situation can be attained in the first part of the reactor where unreacted ammonia is still present along with NO. In line with the hypothesis of the occurrence of a NO-SNCR reaction involving ammonia, the presence of the biogas-derived fuel favors the NO reduction process.

Eventually, our data apparently suggest that it is possible, in principle, to limit the NO emission during the catalytic combustion of NH_3-containing fuels by a proper selection of the operating conditions which favor the occurrence of $DeNO_x$-SNCR processes involving NH_3 as reducing agent. However, the direct extrapolation of our conclusions to real gas turbines operation conditions must be done with caution, in view of the very different operating conditions involved in the two cases (P=10–20 atm vs. atmospheric pressure; O_2=20 vs. 2% v/v; fuel concentration one order of magnitude higher, residence time 10–30 ms vs. about 1 s, presence of sulfur and alkali compounds which can poison the catalysts). As a matter of fact, preliminary experiments performed over pilot-scale catalytic combustors equipped with either hexaaluminate catalysts and/or noble metal-based catalysts apparently indicate that conditions favoring the occurrence of the SNCR process can be hardly established upon the catalytic combustion of biogas [33].

5. Conclusions

The preparation, characterization and reactivity of Me-substituted hexaaluminate catalysts (Me=Mn, Ni, Co, Fe and Cr) in the catalytic combustion of biomasses derived fuels has been investigated in the present study. It has been found that the simple preparation method adopted here, i.e. precipitation from an aqueous solution of the metal ions with ammonium carbonate (carbonate route), results in microcrystalline matrices of high surface areas, in which an high interspersion of the constituents is provided. Calcination at high temperatures (1300°C) allows for the achievement of a final monophasic materials with a Ba–β-Al_2O_3 structure accommodating the Me ion. It has been found that Ni^{2+}, Cr^{3+} and Fe^{3+} are allocated in octahedral sites, whereas Co^{2+} and Co^{3+} are accommodated in tetrahedral and octahedral coordination, respectively. Surface areas of the samples are in the range 5–15 m^2/g.

The formation of the layered Ba–β-Al_2O_3 possibly proceeds through simultaneous solid state reaction

between amorphous Ba species and γ-Al_2O_3 and between $BaAl_2O_4$ with γ-Al_2O_3. A threshold temperature of 1100°C has been found for the formation of Ba–β-Al_2O_3 phase that has been related to the activation of the mobility and diffusion of Ba ions into the γ-Al_2O_3 spinel blocks. However in the case of the Mn-containing samples, the onset of the transformation is seen 100°C below, i.e. near 1000°C. A minor promoting effect on the formation of the final phase is also observed for the Fe-containing catalyst.

All the substituted hexaaluminate catalysts investigated in the present work are active in the catalytic combustion of the biomass-derived fuels. Methane, which is the least active biogas fuel, shows a light-off temperature close to 550°C over both the Fe- and the Mn-substituted hexaaluminate samples, whereas it is converted at slightly higher temperatures over the Ni, Co, and Cr-containing samples. CO and H_2 ignited over all catalyst samples at lower temperatures, i.e. near 300°C, with the exclusion of the Ni-substituted catalyst which shows a very poor reactivity towards CO below 750°C.

Over all the catalyst samples, ammonia contained in the biogas shows a similar reactivity and is oxidized to N_2 and NO. Notably, the NO formation shows a maximum in the range 600–800°C: above this temperature, the concentration of NO is strongly reduced and a corresponding increase in the N_2 concentration is observed. This effect is more evident when the NH_3 oxidation is carried out in the presence of the biogas fuels components. The reduction of the NO concentration at high temperature has been associated with the occurrence of a SNCR process of NO by NH_3, which in line with literature indication is enhanced by the presence of the biogas fuels. The occurrence of the SNCR process requires the simultaneous presence of oxygen, NO and ammonia, a condition which is effectively matched in the first part of the reactor where NH_3 is only partially converted to NO. Such process could be exploited, in principle, to limit the NO emission during the catalytic combustion of NH_3-containing fuels if proper operating conditions are established. As a matter of fact, preliminary experiments performed over pilot-scale catalytic combustors have indicated that conditions which enable the occurrence of the NO-SNCR process can be hardly obtained under actual gas turbine operation.

Acknowledgements

This work has been performed under EC contract JOR3-CT96-0071. The financial support of Ministero dell'Università e della Ricerca Scientifica e Tecnologica (MURST), Rome, Italy, is also acknowledged.

References

[1] J.G. McCarty, in: Proceedings of the EUROPACAT-III, Krakow, Poland, 1997, p. 70.
[2] R. Tucci, Hydrocarbon Process. (1982) 159.
[3] R.B. Anderson, K.C. Stein, J.J. Feenan, L.J. Hofer, Ind. Eng. Chem. 53 (1961) 809.
[4] R. Farrauto, M.C. Hobson, T. Kennelly, E. Waterman, Appl. Catal. A 81 (1992) 227.
[5] R. Burch, F.J. Urbano, Appl. Catal. A 124 (1995) 121.
[6] S.C. Su, J.N. Carstens, A.T. Bell, J. Catal. 176 (1998) 136.
[7] M. Machida, K. Eguchi, H. Arai, J. Catal. 103 (1987) 385.
[8] G. Groppi, E. Tronconi, P. Forzatti, Appl. Catal. A 138 (1996) 177.
[9] G. Groppi, L. Lietti, E. Tronconi, P. Forzatti, Catal. Today 45 (1998) 159.
[10] C. Cristiani, G. Groppi, P. Forzatti, E. Tronconi, G. Busca, M. Daturi, in: Studies on Surface Science and Catalysis, Vol. 101, Elsevier, Amsterdam, 1996, p. 473.
[11] G. Groppi, M. Bellotto, C. Cristiani, P. Forzatti, P.L. Villa, Appl. Catal. A 104 (1993) 101.
[12] H. Sadamori, Catal. Today 47 (1999) 325.
[13] L. Lietti, C. Ramella, G. Groppi, P. Forzatti, Appl. Catal. B 21 (1999) 89.
[14] G. Groppi, C. Cristiani, M. Bellotto, P. Forzatti, J. Mater. Sci. 29 (1994) 3441.
[15] G. Groppi, M. Bellotto, C. Cristiani, P. Forzatti, P.L. Villa, J. Mater. Sci. 34 (1999) 1.
[16] G. Groppi, C. Cristiani, P. Forzatti, J. Catal. 168 (1997) 95.
[17] F.P. Treadwel, Chimica Analitica, 3rd Edition, Vallardi Publisher, Milan, 1966.
[18] J.G. McCarty, M. Gusman, D.M. Lowe, D.L. Hildenbrand, K.N. Lau, Catal. Today 47 (1999) 5.
[19] G. Busca, G. Ramis, M.C. Priedo, V.S. Escribano, J. Mater. Chem. 3 (1993) 665.
[20] G.H. Faye, Can. Mineral. 12 (1974) 389.
[21] C.K. Jørgensen, in: Absorption Spectra and Chemical Bonding in Complexes, Pergamon Press, Oxford, 1962.
[22] W.W. White, G.J. McCarthy, B.E. Scheetz, Am. Mineral. 56 (1971) 72.
[23] R.K. Moore, W.B. White, Can. Mineral. 11 (1972) 791.
[24] M. Machida, K. Eguchi, H. Arai, J. Catal. 120 (1989) 377.
[25] A.F. Wells, in: Structural Inorganic Chemistry, 4th Edition, Clarendon Press, Oxford, 1975.
[26] E.M. Johansson, S.G. Järås, Catal. Today 47 (1999) 359.
[27] P. Glarborg, J.A. Miller, Combust. Flame 99 (1994) 475.
[28] J.E. Johonsson, Fuel 73 (9) (1994) 1398.

[29] R. Laster, F.J. Barnes, R. Mansyczewsky, T.J. Edwards, B.S. Haynes, in: Proceedings of the 24th International Symposium on Combustion, The Combustion Institute Pittsburgh, Pittsburgh, USA, 1992, p. 899.
[30] W. Duo, K. Dam-Johansen, K. Osteraard, in: Proceedings of the 23rd International Symposium on Combustion, The Combustion Institute, Pittsburgh, USA, 1990, p. 297.
[31] M. Jodal, C. Nielsen, T. Hulgaard, K. Dam-Johansen, in: Proceedings of the 23th International Symposium on Combustion, The Combustion Institute, Pittsburgh, USA, 1990, p. 237.
[32] J.A. Caton, J.K. Narney II, C. Cariappa, W.R. Laster, Can. J. Chem. Eng. 73 (1995) 345.
[33] M. Berg, E.M. Johansson, S.G. Järås, Catal. Today 59 (2000) in press.